

Received September 27, 2019, accepted October 27, 2019, date of publication October 29, 2019, date of current version November 14, 2019.

Digital Object Identifier 10.1109/ACCESS.2019.2950375

A Modified Hybrid Maximum Power Point Tracking Method for Photovoltaic Arrays Under Partially Shading Condition

WEI ZHANG¹, GUOPENG ZHOU², HAO NI¹, AND YUNLIAN SUN³

¹School of Electronics and Information Engineering, Hubei University of Science and Technology, Xianning 437100, China

²Institute of Engineering and Technology, Hubei University of Science and Technology, Xianning 437100, China

³School of Electrical Engineering and Automation, Wuhan University, Wuhan 430072, China

Corresponding author: Wei Zhang (zwei1987@yeah.net)

This work was supported in part by the Technical Innovation Special Project (Major Project), Hubei Science and Technology Department of China under Grant 2018ABA076, in part by the Special Project on Capacity Building for Scientific and Technological Innovation and Entrepreneurship Services, Hubei Science and Technology Department of China under Grant 2019BEC206, and in part by the Scientific Research Project, Hubei university of science and technology under Grant 201819x042.

ABSTRACT To ensure the photovoltaic (PV) arrays under partial shading condition (PSC) could still output maximum power quickly and efficiently, this work presents a modified hybrid maximum power point tracking (MPPT) method, which applies artificial neural network (ANN) to the modified perturb and observe (MP&O). Instead of using expensive illumination intensity sensors directly, the illumination intensity on each module in the PV array can be obtained indirectly by sampling the specific points of their own cheaper voltage-current sensors. ANN uses indirect illumination intensity to predict the optimal voltage areas of the global maximum power point (GMPP). Based on the areas, MP&O adopts a adaptive step size strategy to obtain GMPP. By modeling and simulation in Matlab/Simulink, it is shown that the tracking time and efficiency of the proposed method in this work can reach 0.026s and 99.87% respectively. Compared with other methods, the method has faster speed, higher efficiency, smaller fluctuation and lower complexity.

INDEX TERMS ANN, MPPT, MP&O, PSC, PV arrays.

I. INTRODUCTION

In the current background of global energy shortages, as an inexhaustible source of clean energy, solar energy has been widely concerned [1]–[3]. As an effective form of utilizing solar energy, photovoltaic (PV) arrays have achieved great development all over the world. However, the current-voltage (I-V) characteristics of PV arrays are nonlinear and have a unique optimal voltage on the curve of power-voltage (P-V), which produces maximum power point (MPP). The progress of finding the optimal voltage is regarded as maximum power point tracking (MPPT) [4]–[6]. Recent years, MPPT methods, consisting of two general categories, namely traditional methods and intelligent methods, have attracted to domestic and foreign researchers [7], [8]. Although traditional methods, including Incremental Conductance (IC), Perturbation and Observation (P&O), Hill Climbing (HC), etc., could track MPP under uniform illumination smoothly, these methods tend to be limited to local maximum power point (LMPP), not locating global maximum

power point (GMPP) under partial shading condition (PSC) and leading to a mass of power losses [9]–[12]. To overcome these shortcoming, intelligent methods including Genetic Algorithm (GA), Fuzzy Control (FC), Particle Swarm Optimization (PSO), Artificial Neural Network (ANN), etc., are put forward. The superiority of the intelligent methods is that they can search the entire area on the curve of P-V under PSC efficiently. However, intelligent algorithms often have the shortages of poor convergence performance and slow tracking speed [13]–[16]. In order to solve these issues, the modified intelligent algorithms are put forward. Kamal et al. [17] have proposed a online adaptive neuro-fuzzy algorithm that incorporates B-spline function from the conventional neuro-fuzzy. A novel overall distribution (OD) method based on particle swarm optimization has been proposed by Li et al. [18]. Based on excluding the use of random numbers in the velocity equation, Sen *et al.* [19] have presented a modified particle velocity-based particle swarm optimization (MPV-PSO) method eliminating the randomness of the traditional PSO method.

Recent studies have shown that traditional method especially P&O method combined with intelligent method can

The associate editor coordinating the review of this manuscript and approving it for publication was Ganesh Naik¹.

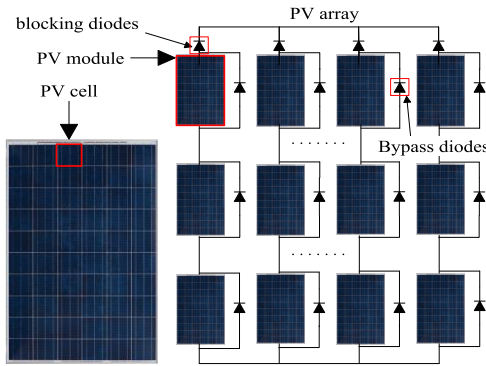


FIGURE 1. Composition of a practical PV array.

not only solve the search problem under PSC effectively, but also improve the tracking efficiency. Jiang *et al.* [20] have presented a hybrid method, which combines conventional and ANN method, from an economic point of view. Goud *et al.* [21] have incorporated the ideas of artificial bee colony (ABC) into single current sensor hill climbing (SSHC) method. Kermadi *et al.* [22] come up with improved algorithm that could minimize the unnecessary movement of particles to faster convergence.

This work presents a modified hybrid MPPT method that combines ANN with MP&O for PV arrays under PSC. Firstly, Instead of using expensive illumination intensity sensors directly, the illumination intensity on each module in the PV array can be obtained indirectly by sampling the specific points of their own cheaper voltage-current sensors. the optimal voltage areas of GMPP is predicted from indirect illumination intensity by ANN. Then based on the location areas, the MP&O adopts a adaptive step size strategy to obtain GMPP. The method can not only be applicable to various PSC patterns, but also can locate GMPP efficiently.

The rest of this work includes: Section II would introduce structure and modeling of PV arrays. Characteristics of PV arrays under PSC would be explained in section III. Section IV would explain the modified hybrid MPPT method in detail. Simulation results and discussion of the proposed method will be presented in section V. Section VI will compare the proposed method with other methods. The conclusion of this work will be drawn in section VII.

II. STRUCTURE AND MODELING OF PV ARRAY

As shown in Fig.1, A PV array is comprised of N_{pp} and N_{ss} modules, connected in parallel and series to obtain high voltage and high current, seeking to improve output power of the PV array. There are two types of diodes in the PV array, which are bypass diodes and blocking diodes. By preventing the shaded module from generating a negative voltage, bypass diodes could eliminate hot-spot phenomenon effectively. Blocking diodes can prevent backward current flow. If some PV cells from modules, or certain modules in the array are shaded at the same time, the PV array is said to be under PSC[23], [24].

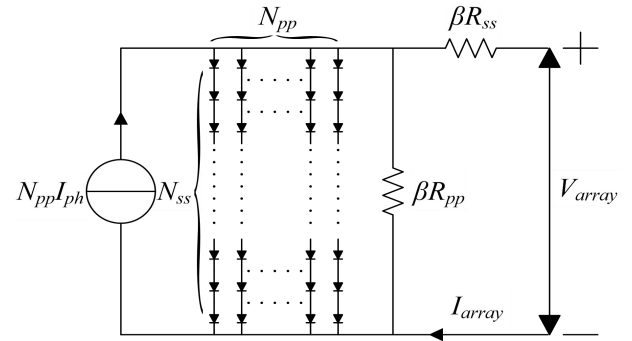


FIGURE 2. Equivalent mode of the single diode.

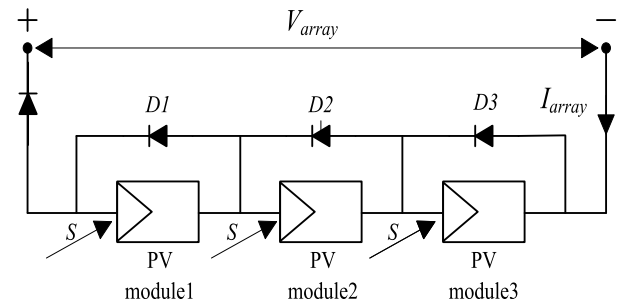


FIGURE 3. Circuit configuration of the PV array under PSC.

In this work, the PV array could be represented by equivalent model of the single diode, depicted in Fig.2. The voltage and current relationship of the PV array can be expressed as[25]:

$$I_{array} = N_{pp}I_{ph} - N_{pp}I_0 \left[\frac{V_{array} + \beta I_{array}R_{ss}}{aV_tN_{ss}} - 1 \right] - \frac{V_{array} + \beta I_{array}R_{ss}}{\beta R_{pp}} \quad (1)$$

$$I_{ph} = \frac{G}{G_N} [I_{ph_N}(1 + R_{ss}/R_{pp}) + K_i(T - T_N)] \quad (2)$$

$$I_0 = \frac{[I_{sc_N} + K_i(T - T_N)]}{\text{Exp}((V_{oc_N} + K_v(T - T_N))/V_t) - 1} \quad (3)$$

where V_{array} and I_{array} are the voltage and current of the PV array respectively. Exp stands for exponent. R_{pp} and R_{ss} are the equivalent parallel resistance and series resistance respectively. I_{ph} and I_0 are the photocurrent of the PV array and saturation current of the diode respectively. N_{pp} and N_{ss} are number of parallel and series. V_t is the diode thermal voltage. a is ideal factor of the diode. β is the ratio of the number in parallel to the number in series (N_{ss}/N_{pp}). I_{ph_N} is the light generated current under standard test condition(STC). T_N and T are standard temperature (25°C) and actual temperature(°C) respectively. G_N and G are standard illumination intensity (1000W/m²) and actual illumination intensity (W/m²) respectively. K_v and K_i are open circuit voltage and short circuit current coefficient respectively. V_{oc_N} and I_{sc_N} are open circuit voltage and short circuit current under STC respectively.

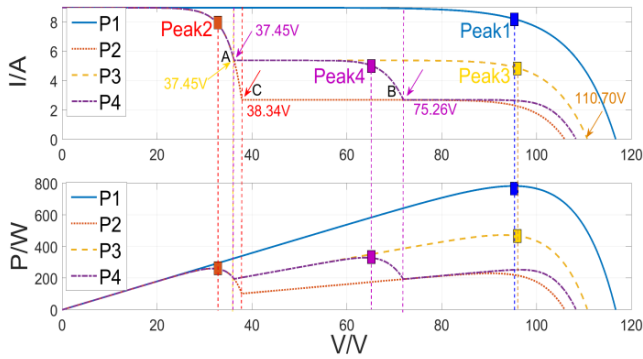


FIGURE 4. Characteristic curves of the PV array under PSC.

TABLE 1. Illumination intensity in this work.

Pattern	Illumination S (W/m ²)		
	PV Module1	PV Module2	PV Module3
P1	1000	1000	1000
P2	1000	300	300
P3	1000	600	600
P4	1000	600	300

III. CHARACTERISTICS OF PV ARRAYS UNDER PSC

As shown in Fig.3, this work would adopt a small PV array made up of three modules in series to illustrate the characteristics of PV array under PSC. The four patterns of the PV array, namely P1, P2, P3, P4, have different illumination intensity, shown in Table I. As a control group, illumination intensity of P1 is under STC. Characteristic curves of the PV array under three patterns are shown in Fig.4.

Under P1, since the PV array works under STC, namely 1000W/m², 1000W/m² and 1000W/m², there is no knee-point on the curve of I-V and only one MPP on the curve of P-V, namely Peak1. Under P2, the illumination intensities of the shaded PV Module2 and the shaded PV Module3 are only 300W/m², while the illumination intensity of the shaded PV Module1 is 1000W/m². The existence of a voltage difference between the PV Module1 and PV Module2 (or the PV Module3) causes conduction of the bypass diode of the PV Module2 and the PV Module3. Therefore, there is one knee-point C on the curve of I-V, where V_C = 38.34V, Meanwhile, the GMPP is positioned at Peak2. Under P3, the illumination intensities of the shaded PV Module2 and the shaded PV Module3 are both 600W/m², while the illumination intensity of the shaded PV Module1 is 1000W/m². There is one knee-point A on the curve of I-V, where V_A = 37.45V, Meanwhile, the GMPP is located at Peak3 clearly. Under P4, the PV Module1, PV Module2 and PV Module3 receive three different illumination intensity, namely 1000W/m², 600W/m² and 300W/m², which brings about two knee-points A and B on the curve of I-V, where V_A = 37.45V and V_B = 75.26V, Meanwhile, the GMPP is located at Peak4.

It can be concluded that different illumination intensity patterns correspond to different current-voltage(I-V) characteristic curves of the PV array, while both the GMPP of the characteristic curves and the number of the knee-point vary from pattern to pattern. Hence, finding the GMPP is very critical.

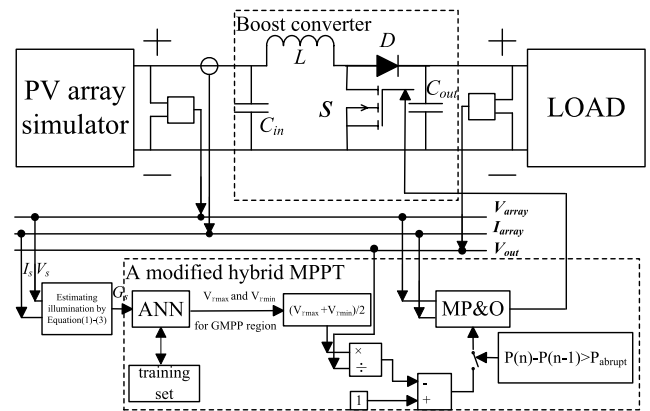


FIGURE 5. Schematic diagram.

TABLE 2. Parameter for the PV module (YGE 60 cell).

Parameter	Value
Optimal power(P _m)	260W
Optimal voltage (V _m)	30.9V
Optimal current (I _m)	8.41A
Open circuit voltage(V _{oc})	38.9V
Short circuit current(I _{sc})	8.98A
K _v	-0.0033V /°C
K _i	0.0006A /°C
Number of cell per module(n)	60

IV. THE PROPOSED MODIFIED HYBRID MPPT METHOD

A. THEORY OF OPERATION

Although ANN have been shown to track GMPP accurately, it has many disadvantages such as difficult of acquiring time-consuming training set, expensive illumination intensity sensors and slow tracking speed [26]–[29]. Based on the above problem, a modified hybrid MPPT method is proposed, dividing into two parts: ANN and MP&O. Assuming that the ambient temperature is maintained at 25°C, the illumination intensity(G_s) on the PV modules is estimated by using the current and voltage of the PV modules instead of illumination intensity sensors, namely using Equation (1)–(3) of Section II to estimating the illumination intensity(G_s) on each module. Schematic diagram is composed of the PV array simulator, boost converter, a modified hybrid MPPT, and load, as shown in Fig.5.

For illustrating the proposed modified hybrid MPPT method, this work uses the small PV array, as described in Fig.3 in section III while parameters for the PV module (YGE 60 cell) are given in Table 2.

The GMPP under different PSC is obtained by changing the illumination intensity on different modules in 100W/m² steps from 100W/m² to 1000W/m²(total 1000 patterns), as shown in Fig.6. As can be seen from Fig.6, GMPP is located in a specific area, namely three optimal voltage areas, and the GMPP of some shaded patterns is consistent(about 415 patterns). The remaining 585 can be used as training set for ANN, which could improve tracking speed.

Based on the above analysis, the basic idea of the method is to predict the optimal voltage areas by ANN, namely V_{rmin} and V_{rmax}, from the illumination intensity on different

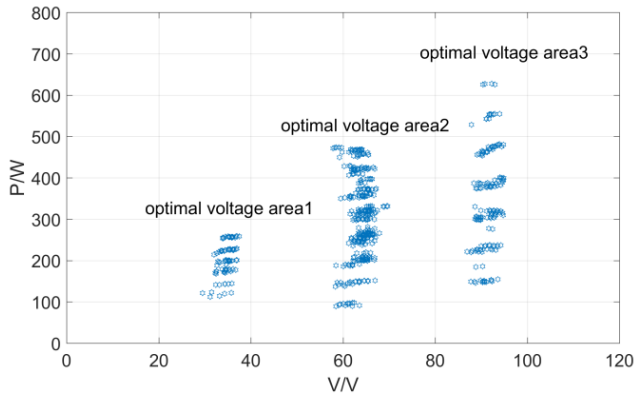


FIGURE 6. GMPP distribution of the PV array under different PSC.

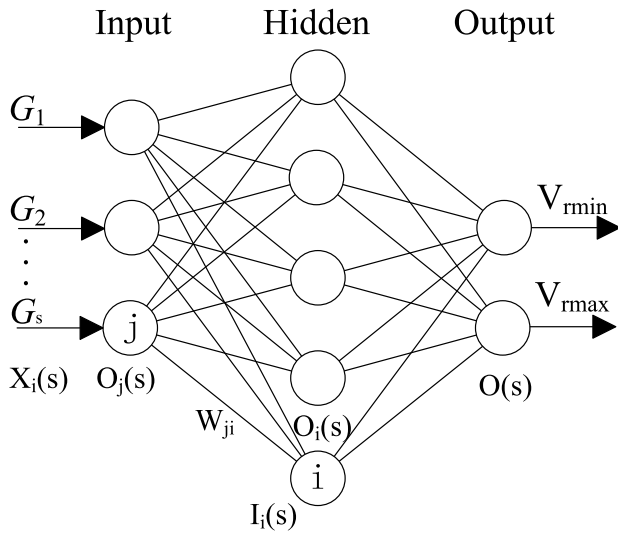


FIGURE 7. Configuration of ANN.

modules, which is estimated by using the current and voltage of the PV modules. Then the MP&O is applied to the areas to achieve the GMPP, using an adaptive step size strategy to reduce the power fluctuation and speed up the tracking process. Hence the proposed method consisting of ANN and MP&O could achieve a better GMPPT performance.

B. ANN SECTION

ANN is used to locate the optimal voltage areas of GMPP. The illumination intensity (G_s) on each module is estimated by using different voltage and current from the sample-point set of I-V curve. As depicted in Fig.7, the configuration of three-layer feed forward ANN has three layers, namely an input layer, a hidden layer, and an output layer. The estimated illumination intensity (G_s) on each module is obtained by the nodes of the input layer, transferred to the hidden layer, which passes their output to the nodes of the output layer, getting the optimal voltage areas of GMPP. The sigmoid function is used for the input-output characteristics of the nodes. For each node j of the input layer and hidden layer, the output $O_j(s)$ is expressed as follows:

$$O_j(s) = \frac{1}{1 + \exp(-X_i(s))} \tag{4}$$

where $X_i(s)$ is the input value to the node j at the s -th sampling, namely G_s .

The input $I_i(s)$ of the hidden layer is expressed by the weighted sum from the previous as follows:

$$I_i(s) = \sum_j W_{ji}(s) * O_j(s) \tag{5}$$

where W_{ji} , set to random values initially, is the weight between node j and i .

For each node i of the hidden layer and output layer, the output $O_i(s)$ is expressed as follows:

$$O_i(s) = \frac{1}{1 + \exp(-I_i(s))} \tag{6}$$

where $I_i(s)$ is the input value to the node i at the s -th sampling.

$$O(s) = \sum O_i(s) \tag{7}$$

where $O(s)$ are the s -th predicted output.

In order to obtain location area accurately, it is very necessary to adjust W_{ji} as training process of the ANN by the function of sum of the squared errors between the target output and the ANN predicted output as follows:

$$e = \sum_{s=1}^N (t(s) - O(s))^2 \tag{8}$$

where N is the total number of training patterns. $t(s)$ and $O(s)$ are the s -th target output and ANN predicted output, respectively. W_{ji} keeps updating so that the error in equation(8) would be reduced.

By adopting Matlab/Simulink to model and simulate PV arrays under different PSC, a large number of output characteristic curve of I-V data sets and the illumination intensity (G_s) on each module could be obtained to train the ANN.

Generally, Levenberg Marquardt (LM) function more suitable for ANN training is adopted where the performance indicator is sum of the squared errors [29]. Since ANN in this work is only used to determine the optimal voltage areas corresponding to GMPP, a slight change of the PV array will not affect the predicted results, so the training data-set can be obtained through Matlab/Simulink, which could greatly simplify the complexity of getting the actual data of the PV array. A lot of training data-set is conducted by ANN through the PV array simulator, which samples the specified point of I-V curve directly [30]. The voltage value of the sample-point set V_s could be set as:

$$V_s = (V_{N_{max}-1}, \dots, V_3, V_2, V_1) \\ V_s = ((i + 0.6)V_{OC_N}, \dots, 2.6V_{OC_N}, 1.6V_{OC_N}, 0.6V_{OC_N}) \tag{9}$$

where $i = 0, 1, 2, \dots, N_{max}-1$. N_{max} is the number of modules in the PV array.

Fig.8 shows the simulation results which could be used for training ANN. The input pattern is the illumination

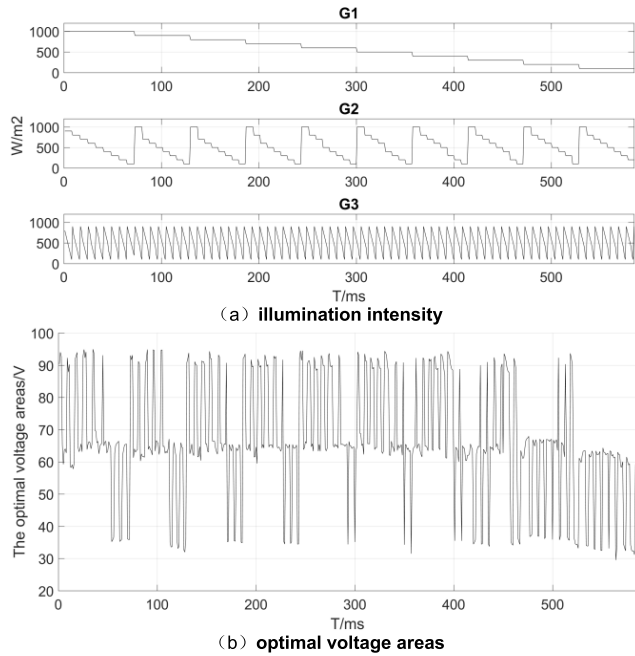


FIGURE 8. Patterns for Training ANN.

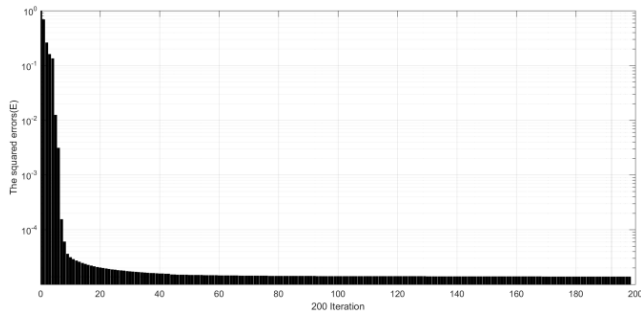


FIGURE 9. Convergence of Error.

intensity(G_s) on each module corresponding to different voltage and current from the sample-point set of I-V curve. The target pattern is given by the optimal voltage areas for training the ANN.

The process of error convergence is shown in figure 9. The ANN was trained by using about 585 pairs of points (Each pattern is made up of three points). During the training process, the squared errors, the learning rate and the momentum are set to 0.001, 0.2 and 0.85 respectively.

C. MP&O section

The MP&O method has used adaptive step size to search the location area and find GMPP ultimately. Through predicting the optimal voltage areas, namely V_{rmin} and V_{rmax} owing GMPP by ANN, GMPP area is located. Both V_{rmin} and V_{rmax} can be used to start the MP&O. V_{rmax} is adopted for the starting search point, and a fixed step size with large correlation is used [31]. But the method often causes the slow search speed and strongly fluctuation. This work uses $(V_{rmax} + V_{rmin})/2$ as a initial searching point, as shown in Fig.5. It could draw a conclusion that the initial searching point is generally located to the left of GMPP in Fig.4. Hence the

TABLE 3. Definition of h.

dV	dP	dV×dP	h
+	+	+	+1
+	-	-	-1
-	-	+	+1
-	+	-	-1

gradient h (negative or positive) of the P-V curve, namely dV and dP could be recorded. The result of symbol multiplication between dV and dP, and normalized to unity, is defined as h which would judge whether the method tracks GMPP, as shown in Table 3.

In this work, seven consecutive recorded values of h are used to estimate whether the power appears to fluctuate. Thus, Absolute value of the sum of h, i.e. |Flag| will occur at

$$|Flag| = \begin{cases} = 7 & \text{the method not converged to stable state} \\ < 7 & \text{the method converged to stable state} \end{cases} \quad (10)$$

As the voltage continues to decrease or increase, seven consecutive values of h would be negative and positive, respectively. Therefore, |Flag| is equal to 7. When GMPP is reached, the power starts to fluctuate. Hence at least three times the voltage move to the opposite direction, leading to |Flag| less than 7. According to the above analysis, fluctuation can be judged by obtaining |Flag|.

In this work, the step size is set as to $2\% \times V_{ref}$, where V_{ref} is equal to $(V_{rmax} + V_{rmin})/2$. When fluctuation is found, the step size decreases $0.5\% \times V_{ref}$ with each generation until it reaches $0.5\% \times V_{ref}$ at stable state, otherwise the step size remains the same. The method could not converge to GMPP strictly, but the adaptive step size is small enough that the fluctuations are negligible, causing small power loss[5]. In fact, the illumination intensity will always fluctuate, so the step size is not allowed to be zero. If a small change in illumination intensity is not enough to cause a change in power, zero step size will cause the method to track the same voltage throughout the cycle and cause sharp fall in power because of the offset in GMPP position. Hence, it is very important to maintain small step size, which could hold a very low fluctuation to reduce power loss rather than zero step size.

D. FLOWCHART OF THE PROPOSED METHOD

The complete flowchart of the proposed method is shown in Fig.10. The sampling points are gained consecutively, i (i = 1,2, ..., $N_{max}-1$) is used to mark the sampling points, and sign ensures that the power error between each sampling point is not affected by an abrupt illumination intensity change.

The basic steps of the proposed method are as follows.

- (a) Initialization: the initial value is set, where $i = N_{max}-1$, $sign = 1$, $N_{max} = 3$, $P_{abrupt} = 50W$, $P(0) = 0W$, $V_s = (0.6 + i)V_{oc}$.
- (b) Input data measurement: the current $I(n)$ and the voltage $V(n)$ are measured, and then power is computed.

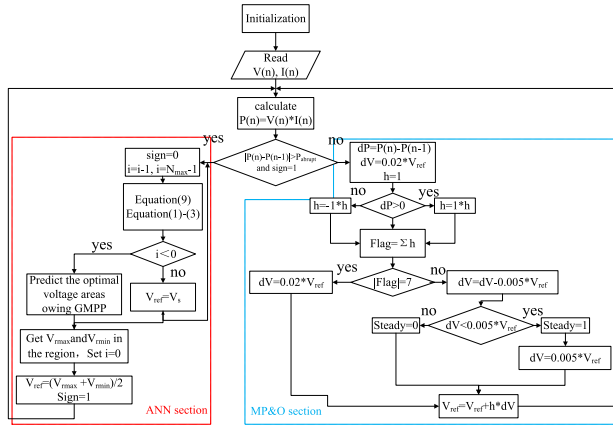


FIGURE 10. Complete flowchart.

- (c) ANN section: the difference between current $P(n)$ and previous power $P(n-1)$ is compared with The critical power variation (P_{abrupt}) . If P_{abrupt} is smaller than the absolute value of the difference, and $sign = 1$, the method starts the searching of the voltage area of GMPP. Primarily, set $sign$ to 0. Then, compute V_s of the I-V curve according to equation(9) for each sampling point i and estimate the illumination intensity (G_s) on each module according to equation(1)–(3), which is exported to the ANN, until $i < 0$. Then the ANN is used to predict the optimal voltage areas owing GMPP and get V_{rmax} and V_{rmin} in the area. The initial V_{ref} is obtained as the key value of the MP&O section, where $V_{ref} = (V_{rmax} + V_{rmin})/2$. Set i and $sign$ to 0 and 1 respectively.
- (d) MP&O section: If P_{abrupt} is bigger than the absolute value of the difference, and $sign = 1$, MP&O section is utilized to track GMPP. The initial step size dV is set to 2% of V_{ref} , while the gradient h , which is the perturbation direction is set to 1. Whether $dP > 0$ is detected. If $dP > 0$, h is equal to h , otherwise h is equal to $-h$. Afterwards, seven consecutive values of h are recorded and $Flag$ is the sum of h . If absolute value $|Flag|$ is equal to 7, it means that the disturbance occurs in the same direction, and the fluctuation around the GMPP has not occurred. At this moment, the step size keeps 2% of V_{ref} . Otherwise If absolute value $|Flag|$ is not equal to 7, the operating point is fluctuating around the GMPP. In this case, the step size decreases with each generation according to 0.5% of V_{ref} , until it arrives at 0.5% of V_{ref} , and GMPP has been found.

V. SIMULATION ANALYSIS AND DISCUSSION

To verify validity of the proposed modified hybrid MPPT method under different PSC, the system is modeled and simulated by Matlab/Simulink as shown in Fig.5. The main parameters of boost converter are as follows: $C_{in} = 100e^{-6}F$, $C_{out} = 300e^{-6}F$, $L = 10e^{-3}H$, $R = 30\Omega$, f_s (witching frequency) = 2000HZ. The configuration of the PV arrays used in simulation is shown in Fig.3, and the parameters is shown in Table 1. P_{abrupt} is set to 50W, and the initial power $P(0)$ is set to 0W. The proposed algorithm is updated every 0.1s.

TABLE 4. Illumination intensity in this work.

PSC Pattern	Illumination S (W/m ²)		
	PV Module1	PV Module2	PV Module3
P1	1000	1000	1000
P2	1000	300	300
P3	1000	600	600
P4	1000	600	300
P5	400	200	300
P6	587	691	345
P7	433	682	229
P8	502	795	312
P9	398	654	213
P10	544	465	865

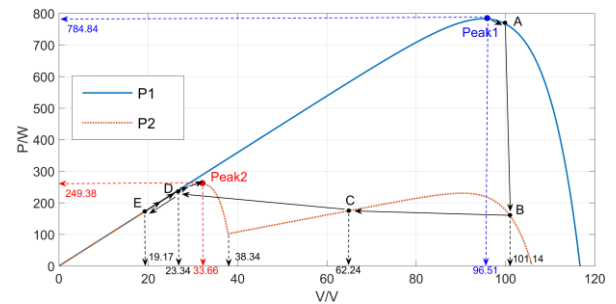


FIGURE 11. The track path of the proposed method when the PSC pattern changes from P1 to P2.

Ten typical PSC patterns are used to verify the method in this work, as shown in Table IV. By the type of illumination, the patterns could be divided into two categories, namely uniform illumination P1 and non-uniform illumination P2 to P10. The pattern of uniform illumination P1 indicates there is a single MPP on the curve of P-V, namely GMPP. However, in the other nine patterns, it is very difficult to track GMPP, because of numerous MPP on the curve of P-V. Four specific cases would be studied, namely P1-P2,P1-P3, P1-P4, P1-P9.

When the system runs at fluctuation point A to the right of the Peak1(GMPP), and the PSC pattern changes suddenly at $T = 1s$, three points are sampled in succession primarily, and then the correlative operating trajectory is A-B-C-D. After the sampling process has been completed, the voltage area of GMPP would be located by ANN, and the midpoint E of the voltage area is finally obtained. As the starting point of MP&O method, the GMPP is tracked rapidly until it has been reached. Fig.11 illustrates the trace path when the PSC pattern changes from P1 to P2. If the PSC pattern changes suddenly, the operating point moves from A to B, and the relative voltage is 101.14V. Then it go through C(62.24V), D(23.34V), E(19.17V) until reaching the Peak2. It is clear that the optimal voltage point was successfully located at 33.66V, while the GMPP could reach 249.38W. The tracking process of the voltage and power are shown in Fig.12 and Fig.13 respectively. It is observed that the power changes from 784.84W to 249.38W, where B, C, D are the corresponding sampling point.

Fig.14 depicts the trace process. If the PSC pattern changes from P1 to P4 suddenly, the execution point moves from A to B, and the relative voltage is 101.14V. Then it go through C(62.24V), D(23.34V), E(49.85V) until reaching the Peak4.

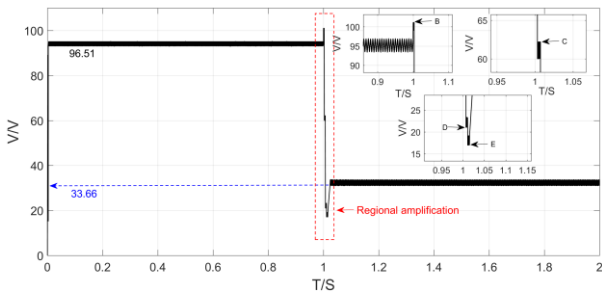


FIGURE 12. The process of the voltage when PSC pattern changes from P1 to P2.

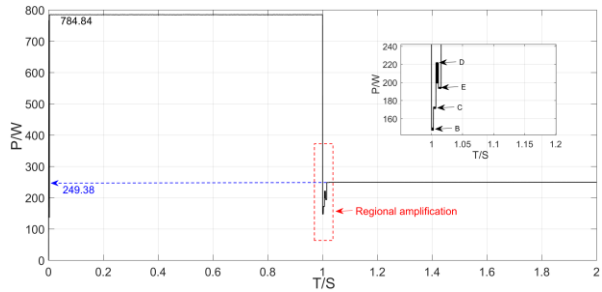


FIGURE 13. The process of the power when PSC pattern changes from P1 to P2.

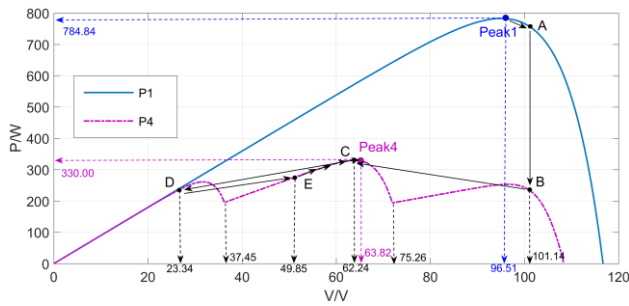


FIGURE 14. The track path of the proposed method when the PSC pattern changes from P1 to P4.

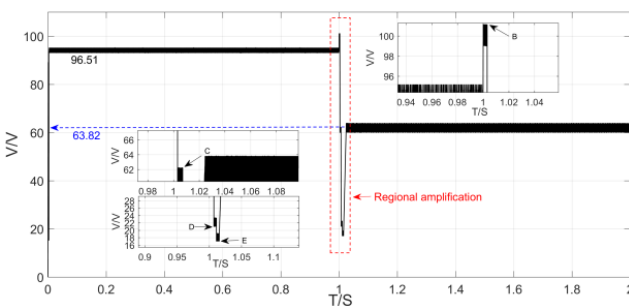


FIGURE 15. The process of the voltage when PSC pattern changes from P1 to P4.

It is indicated that the optimal voltage point was successfully located at 63.82V, while the GMPP could reach 330.00W smoothly. The tracking process of the voltage and power are shown in Fig.15 and Fig.16 respectively. It is observed that the power value changes from 784.84W to 330.00W, where B, C, D are the corresponding sampling point.

Fig.17 illustrates the trace path. If the PSC pattern changes from P1 to P9 suddenly, the operating point moves from A to B, and the relative voltage is 101.14V. Then it go through

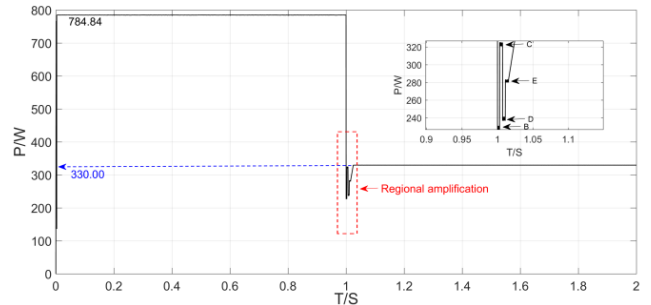


FIGURE 16. The process of the power when PSC pattern changes from P1 to P4.

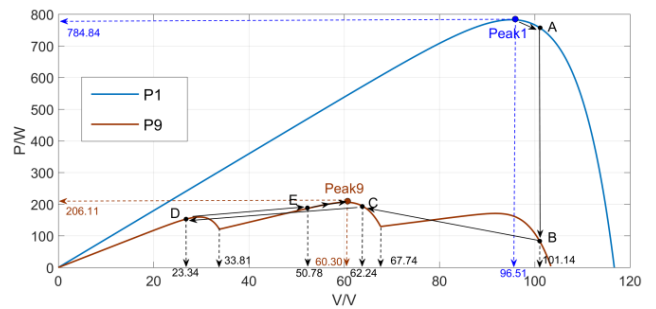


FIGURE 17. The track path of the proposed method when the PSC pattern changes from P1 to P9.

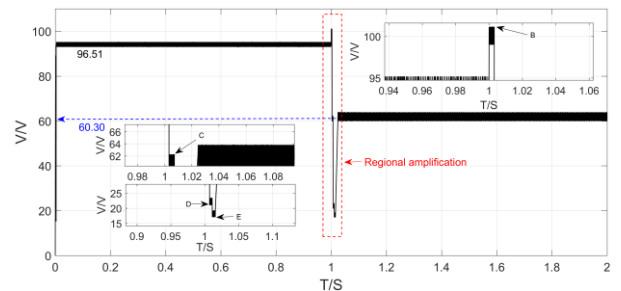


FIGURE 18. The process of the voltage when PSC pattern changes from P1 to P9.

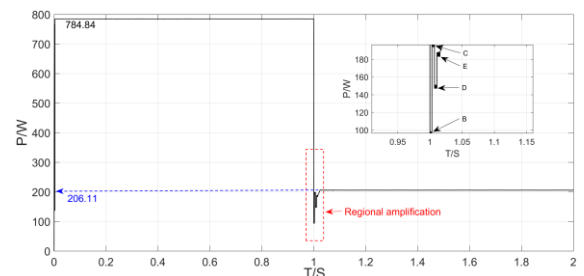


FIGURE 19. The process of the power when PSC pattern changes from P1 to P9.

C(62.24V), D(23.34V), E(50.78V) until reaching the Peak9. It is indicated that the proposed method has tracked to the GMPP at 60.30 V and 206.11W. The tracking process of the voltage and power are shown in Fig.18 and Fig.19 respectively. It can be shown that the power value changes from 784.84W to 206.11W, where B, C, D are the corresponding sampling point.

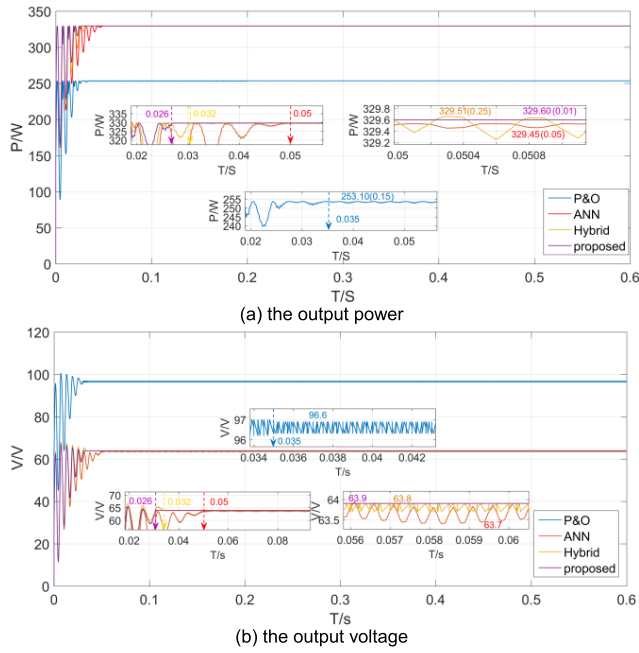


FIGURE 20. Comparison of the output result under P4.

VI. COMPARISON STUDY OF THE PROPOSED METHOD AND OTHER METHODS

To test the performance of the proposed method, the P&O [11], ANN [27] and Hybrid [32] are used for the comparison in this work. The results with the proposed method, the P&O, the ANN and the Hybrid under P4 are carried out, as shown in Fig.20. The illumination of PV modules is shown in Table 1. The curve of P-V is given in Fig.4. It is observed that the relative voltage at the Peak4 is 63.82V and the corresponding power is 330.00W. The average output power P_{av} could be expressed in (11).

$$P_{av} = \frac{\sum_{i=1}^m P_x(i)}{m} \tag{11}$$

where m is the total sampling number, while $P_x(i)$ is the power of the specific method at the i th sampling point.

The output curve of P-T and V-T using the P&O, ANN, Hybrid and the proposed method are shown in Fig.20. In the P&O method, it falls into LMPP at 0.035s where the average output power, voltage and steady state fluctuation are 253.10W, 96.6V and 0.15W respectively. With the ANN method, it takes 0.05s to track GMPP, where the average output power, voltage and steady state fluctuation are 329.45W, 63.7V and 0.05W respectively. The Hybrid Method takes 0.032s to track GMPP, where the average output power, voltage and steady state fluctuation are 329.51W, 63.8V and 0.25W respectively. It takes 0.026s to acquire the GMPP with the proposed method, where the average output power, voltage and steady state fluctuation are 329.60W, 63.9V and 0.01W respectively. Therefore, comparing with the other three methods, the steady state fluctuation of the proposed method is significantly reduced and smoother. Besides, it shows the better MPPT tracking speed than others.

TABLE 5. Performance comparisons of the P&O, ANN, Hybrid and the proposed method.

PSC	Methods	Tracking time(s)	P_{av} (W)	Fluctuation(W)	η (%)	Complexity
P4	P&O	0.035	253.10	0.15	76.79	High
	ANN	0.05	329.45	0.05	99.83	Medium
	Hybrid	0.032	329.51	0.25	99.85	Low
	proposed	0.026	329.60	0.01	99.87	Low

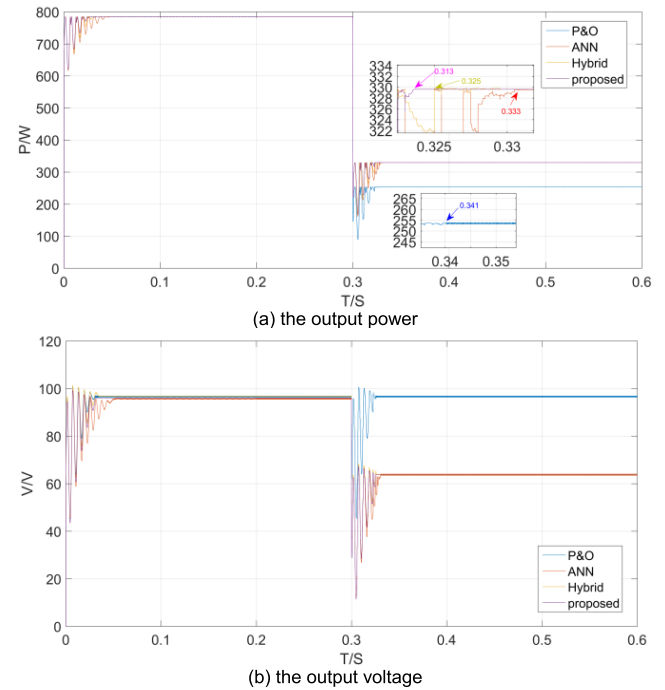


FIGURE 21. Comparison of the output result when PSC pattern changes from P1 to P4.

To contrast the efficiency of the proposed method with others, the efficiency η could be expressed in (12).

$$\eta = \frac{P_{av}}{P_{th}} \times 100\% \tag{12}$$

where P_{th} are the theoretical GMPP.

The efficiency η and average power P_{av} by the P&O, ANN, Hybrid and the proposed method could be obtained, as shown in Table 5. It is shown, except that average power of the P&O is 253.10W which located at LMPP, P_{av} is 329.45W, 329.51W and 329.60W of the three MPPT methods, while the efficiency is 99.83%, 99.85% and 99.87% respectively. Through the above simulation, The proposed method has excellent performance in tracking speed, efficiency and reducing fluctuation.

By comparing the complexity of the methods, it can be seen that except the hybrid method, the proposed method can effectively reduce the unnecessary search process and the dimension, which is obviously lower than the other two methods.

In view of the rapid change of illumination intensity, the proposed method is compared with other methods in tracking time, as shown in Fig.21. Fig.21 shows the dynamic change in the output power and the output voltage when the PSC pattern changes from P1 to P4 at 0.3 seconds. In the P&O method, It takes 0.341 seconds to reach the LMPP(253.1W). With the ANN method, 0.333 seconds is needed to reach the GMPP(329.45W). The Hybrid Method takes 0.325s to obtain the GMPP(329.51W). The proposed method only needs 0.313 seconds to obtain the GMPP(329.6W). It can be clearly shown that the proposed method has better dynamic tracking performance than other methods.

The above experimental results are limited to PV arrays with only three modules, but the modified proposed hybrid MPPT method could be easily extended to more modules in series of larger PV arrays. The successful application of the method depends on the structure of ANN. For small and medium scale PV arrays, simple ANN can be adopted, such as the feed forward ANN and widely used back propagation. For large-sized PV arrays, a complicated ANN should be constructed, or it is divided into several small and medium scale distributed PV arrays to prevent the application of MPPT of the centralized large-sized PV arrays under PSC from large loss of output power.

VII. CONCLUSION

The characteristic curve of PV arrays under PSC presents multiple peaks. For traditional and intelligent methods, there are more or less problems with accuracy and tracking speed. A modified proposed hybrid MPPT method for PV arrays under PSC are proposed for reducing the tracking range based on study of characteristics of PV arrays. The proposed method consists of two sections: ANN and MP&O. Not needing expensive illumination intensity sensors, the ANN is capable of predicting the optimal voltage areas owing GMPP by sampling the specified point of the current-voltage (I-V) curve. Then based on the location area, the MP&O is used by adopting adaptive step size which could reduce system fluctuation and track GMPP quickly. The simulation analysis and comparison with others have demonstrated the validity of the proposed method. The tracking time and efficiency of the proposed method can reach 0.026s and 99.87% respectively. The proposed method has excellent performance in tracking speed, efficiency and reducing fluctuation.

REFERENCES

- [1] S. Selvakumar, M. Madhusmita, C. Koodalsamy, S. P. Simon, and Y. R. Sood, "High-speed maximum power point tracking module for PV systems," *IEEE Trans. Ind. Electron.*, vol. 66, no. 2, pp. 1119–1129, Feb. 2019.
- [2] M. Seyedmehmoudian, B. Horan, T. K. Soon, R. Rahmani, A. M. T. Oo, S. Mekhilef, and A. Stojcevski, "State of the art artificial intelligence-based MPPT techniques for mitigating partial shading effects on PV systems—A review," *Renew. Sustain. Energy Rev.*, vol. 64, pp. 435–455, 2016.
- [3] E. I. Batzelis, S. A. Papanthassiou, and B. C. Pal, "PV system control to provide active power reserves under partial shading conditions," *IEEE Trans. Power Electron.*, vol. 33, no. 11, pp. 9163–9175, Nov. 2018.
- [4] J. Ahmed and Z. Salam, "A modified P&O maximum power point tracking method with reduced steady-state oscillation and improved tracking efficiency," *IEEE Trans. Sustain. Energy*, vol. 7, no. 4, pp. 1506–1515, Oct. 2016.
- [5] M. Killi and S. Samanta, "Modified perturb and observe MPPT algorithm for drift avoidance in photovoltaic systems," *IEEE Trans. Ind. Electron.*, vol. 62, no. 9, pp. 5549–5559, Sep. 2015.
- [6] W. Zhu, L. Shang, P. Li, and H. Guo, "Modified hill climbing MPPT algorithm with reduced steady-state oscillation and improved tracking efficiency," *J. Eng.*, vol. 2018, no. 17, pp. 1878–1883, Nov. 2018.
- [7] S. Lyden, M. E. Haque, A. Gargoom, and M. Negnevitsky, "Review of maximum power point tracking approaches suitable for PV systems under partial shading conditions," in *Proc. Australas. Univ. Power Eng. Conf. (AUPEC)*, Hobart, TAS, Australia, Sep./Oct. 2013, pp. 1–6.
- [8] B. Subudhi and R. Pradhan, "A comparative study on maximum power point tracking techniques for photovoltaic power systems," *IEEE Trans. Sustain. Energy*, vol. 4, no. 1, pp. 89–98, Jan. 2013.
- [9] N. Kumar, I. Hussain, B. Singh, and B. K. Panigrahi, "Self-adaptive incremental conductance algorithm for swift and ripple-free maximum power harvesting from PV array," *IEEE Trans. Ind. Informat.*, vol. 14, no. 5, pp. 2031–2041, May 2018.
- [10] K. S. Tey and S. Mekhilef, "Modified incremental conductance algorithm for photovoltaic system under partial shading conditions and load variation," *IEEE Trans. Ind. Electron.*, vol. 61, no. 10, pp. 5384–5392, Oct. 2014.
- [11] S. K. Kollimalla and M. K. Mishra, "Variable perturbation size adaptive P&O MPPT algorithm for sudden changes in irradiance," *IEEE Trans. Sustain. Energy*, vol. 5, no. 3, pp. 718–728, Jul. 2014.
- [12] X. Xiao, X. Huang, and Q. Kang, "A hill-climbing-method-based maximum-power-point-tracking strategy for direct-drive wave energy converters," *IEEE Trans. Ind. Electron.*, vol. 63, no. 1, pp. 257–267, Jan. 2016.
- [13] Syafaruddin, T. Hiyama, and E. Karatepe, "Investigation of ANN performance for tracking the optimum points of PV module under partially shaded conditions," in *Proc. Conf. IPEC*, Singapore, Oct. 2010, pp. 1186–1191.
- [14] Y. Wang, Y. Li, and X. Ruan, "High-accuracy and fast-speed MPPT methods for PV string under partially shaded conditions," *IEEE Trans. Ind. Electron.*, vol. 63, no. 1, pp. 235–245, Jan. 2016.
- [15] S. Tang, Y. Sun, Y. Chen, Y. Zhao, Y. Yang, and W. Szeto, "An enhanced MPPT method combining fractional-order and fuzzy logic control," *IEEE J. Photovolt.*, vol. 7, no. 2, pp. 640–650, Mar. 2017.
- [16] R. B. A. Koad, A. F. Zobaa, and A. El-Shahat, "A novel MPPT algorithm based on particle swarm optimization for photovoltaic systems," *IEEE Trans. Sustain. Energy*, vol. 8, no. 2, pp. 468–476, Apr. 2017.
- [17] T. Kamal, M. Karabacak, S. Z. Hassan, H. Li, and L. M. Fernández-Ramírez, "A robust online adaptive B-spline MPPT control of three-phase grid-coupled photovoltaic systems under real partial shading condition," *IEEE Trans. Energy Convers.*, vol. 34, no. 1, pp. 202–210, Mar. 2019.
- [18] H. Li, D. Yang, W. Su, J. Lü, and X. Yu, "An overall distribution particle swarm optimization MPPT algorithm for photovoltaic system under partial shading," *IEEE Trans. Ind. Electron.*, vol. 66, no. 1, pp. 265–275, Jan. 2019.
- [19] T. Sen, P. Nataraj, V. Argawal, and R. Kumar, "Global maximum power point tracking of PV arrays under partial shading conditions using a modified particle velocity-based PSO technique," *IET Renew. Power Gener.*, vol. 12, no. 5, pp. 555–564, Dec. 2017.
- [20] L. L. Jiang, D. R. Nayanasiri, D. L. Maskell, and D. M. Vilathgamuwa, "A simple and efficient hybrid maximum power point tracking method for PV systems under partially shaded condition," in *Proc. 39th Annu. Conf. IEEE Ind. Electron. Soc. (IECON)*, Vienna, Austria, Nov. 2013, pp. 1513–1518.
- [21] J. S. Goud, R. Kalpana, and B. Singh, "A hybrid global maximum power point tracking technique with fast convergence speed for partial-shaded PV systems," *IEEE Trans. Ind. Appl.*, vol. 54, no. 5, pp. 5367–5376, Sep./Oct. 2018.
- [22] M. Kermadi, Z. Salam, J. Ahmed, and E. M. Berkouk, "An effective hybrid maximum power point tracker of photovoltaic arrays for complex partial shading conditions," *IEEE Trans. Ind. Electron.*, vol. 66, no. 9, pp. 6990–7000, Sep. 2019.
- [23] J. Ahmed and Z. Salam, "An improved method to predict the position of maximum power point during partial shading for PV arrays," *IEEE Trans. Ind. Informat.*, vol. 11, no. 6, pp. 1378–1387, Dec. 2015.

- [24] H. Patel and V. Agarwal, "MATLAB-based modeling to study the effects of partial shading on PV array characteristics," *IEEE Trans. Energy Convers.*, vol. 23, no. 1, pp. 302–310, Mar. 2008.
- [25] A. Mäki and S. Valkealahti, "Power losses in long string and parallel-connected short strings of series-connected silicon-based photovoltaic modules due to partial shading conditions," *IEEE Trans. Energy Convers.*, vol. 27, no. 1, pp. 173–183, Mar. 2012.
- [26] E. Karatepe and T. Hiyama, "Artificial neural network-polar coordinated fuzzy controller based maximum power point tracking control under partially shaded conditions," *IET Renew. Power Gener.*, vol. 3, no. 2, pp. 239–253, 2009.
- [27] R. Subha and S. Himavathi, "Neural network based maximum power point tracking scheme for PV systems operating under partially shaded conditions," in *Proc. Int. Conf. Adv. Green Energy (ICAGE)*, Thiruvananthapuram, India, Dec. 2014, pp. 39–43.
- [28] P. Q. Dzung, L. D. Khoa, H. H. Lee, L. M. Phuong, and N. T. D. Vu, "The new MPPT algorithm using ANN-based PV," in *Proc. Int. Forum Strategic Technol.*, Ulsan, South Korea, 2010, pp. 402–407.
- [29] C. Wei, Z. Zhang, W. Qiao, and L. Qu, "An adaptive network-based reinforcement learning method for MPPT control of PMSG wind energy conversion systems," *IEEE Trans. Power Electron.*, vol. 31, no. 11, pp. 7837–7848, Nov. 2016.
- [30] M. A. Ghasemi, A. Ramyar, and H. Iman-Eini, "MPPT method for PV systems under partially shaded conditions by approximating I–V curve," *IEEE Trans. Ind. Electron.*, vol. 65, no. 5, pp. 3966–3975, May 2018.
- [31] H. M. El-Helw, A. Magdy, and M. I. Marei, "A hybrid maximum power point tracking technique for partially shaded photovoltaic arrays," *IEEE Access*, vol. 5, pp. 11900–11908, 2017.



WEI ZHANG was born in Xianning, Hubei, China, in 1987. He received the B.S. degree from the Hubei University of Technology, in 2011, and the M.Sc. degree from Wuhan University, Wuhan, China, in 2013, all in electrical engineering.

From 2013 to 2017, he was a Work Leader of Changde Power Supply Company of State Grid. He has been an Engineer with the Hubei University of Science and Technology, since 2017. His research interests include renewable energy generation and stability, and power quality of renewable energy.



GUOPENG ZHOU was born in Xianning, Hubei, China, in 1972. He received the B.S. degree in fundamental mathematics from Hubei University, Wuhan, China, in 1994, and the M.Sc. and Ph.D. degrees in mathematics and applied mathematics from the South China University of Technology, Guangzhou, China, in 2008, respectively.

He is currently a Professor with the Hubei University of Science and Technology, Xianning. His research interests include power system operation and control and industrialization of photovoltaic system.



HAO NI was born in 1981. He received the M.S. degree from the College of Teacher Education, Zhejiang Normal University, Jinhua, Zhejiang.

He is currently an Associate Professor with the Hubei University of Science and Technology. His current research interests accumulate in the area of machine learning, computer vision, and 2-D material simulation and calculation.



YUNLIAN SUN was born in Wuhan, Hubei, China, in 1962. She received the B.S. degree in radio communication from Peking University, Beijing, China, in 1984, and the M.Sc. and Ph.D. degrees in power system automation from Wuhan University, Wuhan, Hubei, China, in 1989 and 1999, respectively.

She is currently a Professor with Wuhan University. Her research interests include renewable energy generation and modern signal-processing applications in power systems.

• • •